Large Eddy Simulation Analysis of Three-dimensional Flow Characteristics of Pump Turbine during Load Increase and Decrease

Hu Xiucheng, Zhang Lixiang

School of Architecture and Engineering, Kunming University of Technology, Kunming, Yunnan 650500）

Abstract: LES (Large Eddy Simulation) is used to carry out 3-D unsteady numerical simulation of pump turbine's load increase and decrease transition process. Various vortex structures in the blade passage with different opening degrees are captured, vortex distribution in the blade passage is displayed, flow structure change characteristics in turbine and pump operating regions with low flow rate are analyzed, relationship between attack angle and blade passage vortex structure is revealed, different forms of blade passage vortex are studied, horseshoe vortex identification variables are proposed, and turbine operating conditions and pump operating conditions vortex structure change characteristics are compared. " The calculation shows that the hydraulic stability of the pump-turbine is closely related to the flow structure characteristics when the operating conditions of the unit are changed. During the load increase and decrease transition process, the size and distribution range of the vane vortex structure change greatly with time, which is the main factor affecting the great change of flow pattern.

Keywords: pump turbine; Large eddy simulation; The transition process; Foliage vortex; flow characteristic

Research background

The inside of pump turbine is a complex turbulent flow with universality and particularity, while the S inversion flow, static and dynamic interference flow,

Working condition change flow and vane rotating shear flow are the current research focuses. Li Jun et al S is simulated by CFD method

The flow field characteristics in the U-shaped region are analyzed. You Guanghua, etc A guide vane asynchronous pre-opening device (MGV device) is used to improve the S shaped flow characteristics.

The stability of the unit operation is enhanced. However, improving the unstable MGV device also has some drawbacks, such as Liu and so on.

Discovery Adoption

The pressure fluctuation amplitude of MGV device is 2 times of that of synchronous guide vane, and the flow instability phenomenon is also significantly increased. Xiao

It is found that MGV breaks the symmetry of the flow field, makes the flow more complicated, and increases the amplitude of pressure pulsation to a certain extent. Tao Ran And Wang Huanmao, etc.

The hump characteristics of the pump are analyzed. Hasmatuchi etc.

Special images are used to inject bubbles between the guide vane and the runner.

The superposition technique observed the stall pattern in the guide vane runner under braking condition, and the measured stall speed was about 70% of the rated speed. Xia Linsheng et al

The SST-SAS turbulence model is used to numerically analyze different working conditions in the four quadrants of a pump turbine with low specific speed under the same opening by using a three-dimensional unsteady numerical simulation method.

In general, there are 5 basic operation modes for power system dispatching, such as static operation, power generation, phase adjustment in power generation direction, and equal adjustment in water pumping and pumping directions. There are more than 20 kinds of operation mode changes and combinations between each mode. The operation mode changes several times a day, even several times an hour. In the process of load increase and decrease during the change of working conditions, because the great change of flow pattern may induce severe coupled vibration of pumped storage system, relevant analysis and research are of great significance for the safe and stable operation of pumped storage system. Under the current technical conditions, large eddy simulation (large-ed dy simulation, LES)

is undoubtedly the most potential and realizable turbulent flow numerical simulation method for turbulent flow numerical simulation problems with complex geometric space and high Reynolds number, such as hydraulic machinery. This article uses the commercial software ANSYS

[9-13]

FLUENT17.1, using LES turbulence model

For the transition process rail of a pump turbine from rated turbine condition to rated pump condition

Three-dimensional unsteady numerical simulation was carried out for the flow states corresponding to 10 operating points on the trace, and the flow structure change characteristics under low flow conditions were analyzed to explore the relationship between the change of operating conditions and the change characteristics of unstable flow structures.

Calculation method

Calculation Area and Grid Design This paper takes a pump turbine as a simulation object, and its main parameters are: runner diameter 4678.5 mm,

The runner inlet height is 656.25 mm, the rated speed is 300 r/min, the rated head is 200 m, and the guide vanes are under rated turbine and pump conditions.

The degrees are 23 and 22 respectively. As shown in figure 1 , the calculation area includes volute area, water guide mechanism area (19 fixed guide vanes and 20 movable guide vanes with negative curvature), runner area (7 vanes) and draft tube area.

According to the flow characteristics of different regions and the characteristics of large-scale parallel computation, grid design and partition are carried out. The fluid-solid interface is a non-slip interface. Sliding interfaces are arranged on the dynamic and static interfaces formed by the rotating regions of the rotating wheels. HyperMesh is adopted to realize grid partition of each region. The volute shell area (except nose end), the water guide mechanism area and the draft tube area are divided into structural grids, while the other areas are divided into tetrahedral unstructured grids with strong adaptability. The maximum grid size of the water guide mechanism area and the runner area is controlled not to exceed 15 mm, wherein the grid size of the blade passage and the near-wall area is controlled not to exceed 6 mm, and the distance y^+ from the wall surface of the first layer grid is less than or equal to 25; The grid size of volute inlet area and draft tube area shall not exceed 40 mm and 50 mm respectively. According to this principle, each calculation area is divided to form a basic grid scheme a, with a total number of cells of 19,685,714. the local area grid is shown in figure 2 .

In order to check the rationality of grid design, based on grid scheme A, 1 times and 2 times encryption methods are adopted respectively to form grid schemes B and C. The rated turbine working condition is taken as the grid inspection and calculation working condition, and the numerical results of the pressure distribution on the blade pressure surface and the runner water torque are compared to judge the rationality of the grid. Through comparison, the calculation results of grid scheme B and C are very close, and the difference of runner water torque is only 0.49%, so grid scheme B is selected as the numerical calculation grid in this paper.

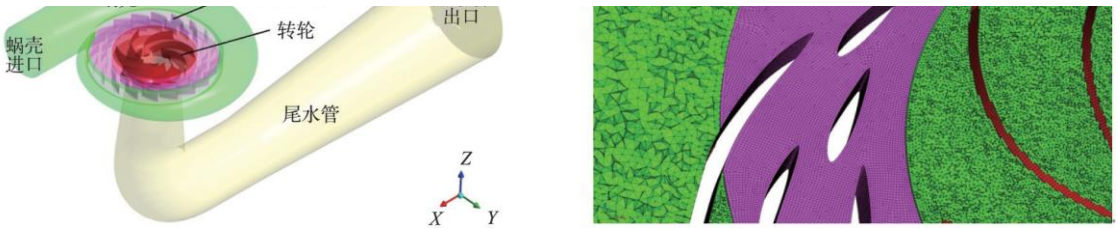

Figure 1 Calculation Area Map 2 Grid Profile at Guide Vane Center

Calculation Method and Initial Conditions selects the large eddy simulation Smagoringsky-Lilly sub-grid stress dynamic mode, which overcomes the shortcomings of the classical Smagorinsky conventional mode. Under the principle of B grid scale, the finite volume method in body-fitted coordinates and non-staggered grid technology are used for spatial discretization. The second-order fully implicit scheme is used for time discretization, in which the convection term adopts the second-order welcome style, and the source term and diffusion term adopt the second-order central scheme.

The calculation of load increase and decrease transition process from turbine operation to pump operation is set according to the way of changing the opening of guide vane at a given speed. The working condition of the water turbine adopts a flow rate inlet and a pressure outlet; The pump adopts quality inlet and free flow. Select 5 water turbine operating points and 5 water pump operating points on the transition process trajectory line for unsteady calculation. The parameters are shown in Table 1 , where Pn is the rated operating condition.

	C				
			O		
	1	2	5	7	1
Guide Vane	1	3	5	6	8
turbine	1	2	3	4	6
pump condition	2	6	8	1	1

Steady calculation shall be carried out for each working condition, and the steady calculation result shall be taken as the initial condition for unsteady calculation. Considering the rotating speed of the runner and
[14]
The calculation scale determines that each rotation of the wheel 1.5° (equivalent to 0.833 ms) is taken as 1 time steps, i.e. 240 is calculated for each rotation of the wheel.
Each time step converges the residual target value 0.001. The calculation duration is considered as 7 rotation cycles, and the 6 that has been stabilized is selected.

Period (*t*) calculation results 6 *t* moment for analysis. Due to the large scale of calculation, the PowerCube-S01 cloud cube of Kunming University of Technology is used.

A certain number of CPU cores in Humber's high-performance computing system perform parallel computation. Due to the fact that the computation efficiency decreases when too many cores are selected for parallel computation of different scales, 60 CPU cores in node 1 are selected for parallel computation. The calculation of each working condition requires about 72 ~ 96 h,

The calculation takes about 720 h in total.

Calculation Results and Analysis

Figure 3—-Figure 8 of Transient Process of Load Reduction in Hydraulic Turbine Working Conditions is the vortex core diagram in the flow passage of hydraulic turbine under each working condition, and each vortex core diagram is of large vorticity.

Vortex core at small 0.1 . When the rated working condition of the turbine is 100 %Pn, the pressure and velocity distribution of the fluid are relatively uniform before the water flow enters the runner, and

The tip of the guide vane is slightly impacted, as shown in fig. 3 , resulting in a small amount of vortex structure development near the tip of the guide vane. When the water enters the runner, the velocity gradient changes sharply, and the turbulence is gradually intense. Theoretically, the runner inlet water flow velocity is basically the same as the tangential direction of the runner inlet blade bone line under the rated working condition of the turbine, i.e. no impact inlet condition is met when the optimal working condition is close to being met, but due to the influence of static and dynamic interference and the like, there is a small angle of attack. The water flows into the blade passage along the inner arc and back arc of the blade after being blocked by the blade leading edge. Under the joint influence of the viscous effect of the curved surface of the three-dimensional twisted blade and the reverse pressure gradient caused by the protrusions, the flow generates flow separation on the curved surface, forming shedding on the suction surface of the blade, instability of the flow pattern, and the vortex generated by shedding forms a complex vortex structure in the blade passage, namely the blade passage vortex. As shown in fig. 3 , the vane vortex consists of a series of vortices of different scales, occupying about the space of the vane 1/3 . Vane vortices flow downstream along the suction surface, converge, interfere with each other, and continuously cascade into many small-scale vortices. The wat flows

Figure 3 Turbine

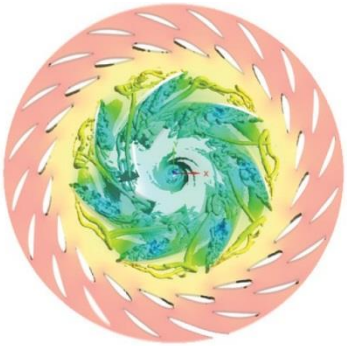

:tion and the elbow section of

Figure 4

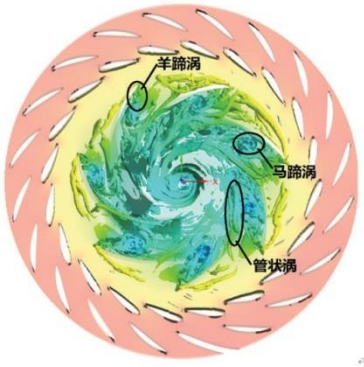

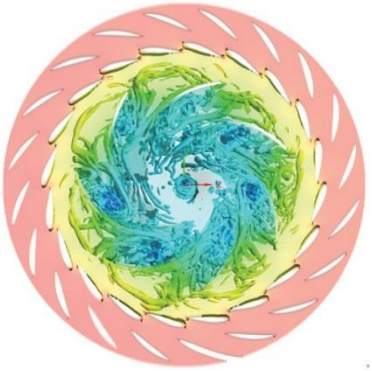

Fig. 5 turbine working condition 50%Pn runner inner vortex core fig. 6 turbine working condition 25%Pn runner inner vortex core

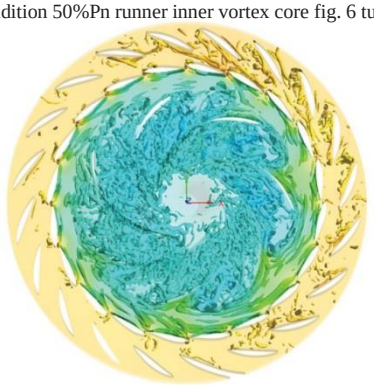

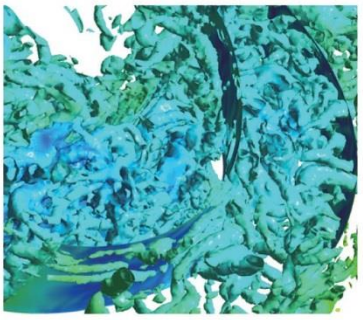

The flow state changes rapidly and finally tends to be uniform in the diffusion section. As the opening of the guide vane decreases, the flow rate decreases, the angle of attack of the flow to the blade end increases, and the impact with the guide vane end increases

The flow separation is becoming more and more obvious, the size of the vane vortex increases, and the distribution of the tubular vortex and horseshoe vortex in the vane is very obvious, indicating that the flow pattern is unstable, as shown in figure 4 and figure 5 . As the opening of the guide vane further decreases, the flow passage between the movable guide vanes is limited, the flow pattern in the runner is disordered and intensified, the streamline is intertwined and disorganized, the vortex scale of the vane passage is relatively small but the space range is wide, and the flow pattern distribution among the vane passages is obviously asymmetrical. As shown in fig. 7 and fig. 8 , when the turbine is operating at 1 %Pn, there are even relatively more vortex structures in the water guide mechanism area. the vortex structures in the runner inner runner are small in size but relatively uniform, and almost occupy the entire runner runner space. there are many vortex bands near the lower ring side at the blade outlet water. the runner outlet water flow does not meet the normal outlet conditions. under the action of the circumferential component of the absolute velocity of the water flow, there is a low pressure in the center of the draft tube and an eccentric draft tube vortex band is formed. in addition, there are phenomena such as backflow in the draft tube diffusion section.

As shown in fig. 9 , 5 virtual surfaces with the same shape and size as the blade surface are arranged in one of the blade passages. the distribution of vortices on these 5 surfaces is observed respectively, such as near wall surface S1 of the blade pressure surface, S2 of the blade passage space 1/4 , S3 of the blade passage middle surface, S4 of the blade passage space 3/4 , and near wall surface S5 of the blade suction surface, so as to reveal the evolution rule of vortices in the blade passage. For the convenience of observation, the vortex structure can be generally divided into two components: the streamwise vortex and the spanwise vortex. However, due to the three-dimensional twisted space inside the runner and the complicated flow direction of the flow field, it is difficult to decompose the vortex into streamwise vortex and spanwise vortex. Therefore, the average vorticity value is used for comparative analysis in this paper. As shown in Figure 10—-Figure 15 , the distribution of vortex cores near each virtual surface under the turbine operating condition of 50 %Pn, and as shown in Figure 16 , the average vorticity of the virtual surface under the turbine off-design condition. It can be seen that, except for the 1 %Pn turbine operating conditions, the virtual surface vorticity lines for all other off-design operating conditions are tubular fishhook type, the average vorticity value of the blade suction surface near the wall S5 is the largest, the blade pressure surface near the wall S1 is the second, and the rest are S4, S3 and S2 in sequence. The larger the average vorticity value is, the more vortex structures there are in the region. The vortex structures near the suction surface are the most, which indicates that the flow separation near the suction surface is relatively significant. The evolution of vortex structure is accompanied by energy dissipation, which can be defined as vortex energy dissipation coefficient $I = w_e$ and $q \times h$, w_e represents vortex energy, q represents flow rate, *and* h "represents water head. The calculation shows that under the same water head, 1 %Pn turbine condition has the largest vortex energy dissipation coefficient, and the rest is 25 %Pn turbine condition, 50 %Pn turbine condition and 75 %Pn turbine condition in sequence. It can be seen from this: the smaller the opening, the greater the vortex energy dissipation coefficient, and the greater the vortex structure energy loss.

According to the above analysis and the structural distribution as shown in Figure 3—-Figure 8 , the structure and distribution characteristics of the vortex system in the blade passage under different opening degrees of the turbine are shown. It can be seen from the figure that the vortex system structure in the runner passage is different at different attack angles. When the angle of attack is small, the stable spiral point develops into a smaller vortex structure in the blade passage, which is similar to the claw vortex and promotes the asymmetric development of the main vortex. When the angle of attack is large, it develops into horseshoe vortex, which restrains the asymmetric development of main vortex by restraining the core of main vortex. As the angle of attack continues to increase, it evolves into a complex multi-vortex system (called the main vortex system). as shown in fig. 7 , it includes not only the main vortex but also the complex secondary vortex structure. for the unsteady horseshoe vortex system, it also includes vortex structures of various unsteady motion modes. When the angle of attack is medium, both horn vortex, horseshoe vortex

and tubular vortex are formed in the blade passage.

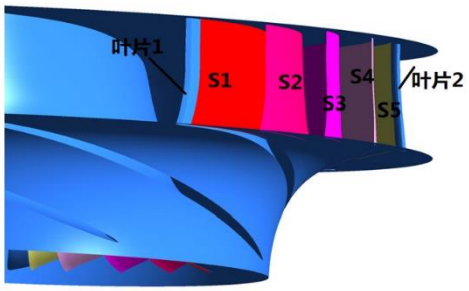

Figure

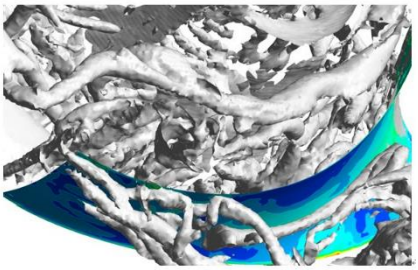

Figure 10 Turbine

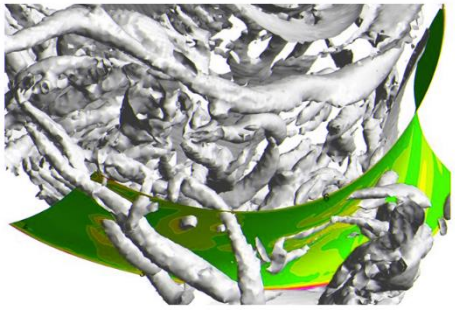

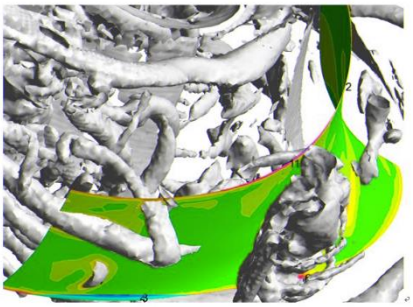

Fig. 11 vortex core near surface S2 at 50%Pn of turbine operation fig. 12 vortex core near surface S3 at 50%Pn of turbine operation

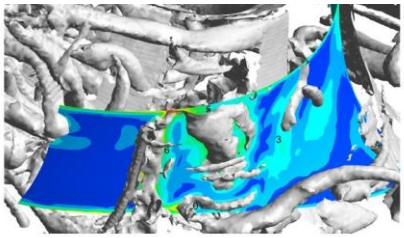

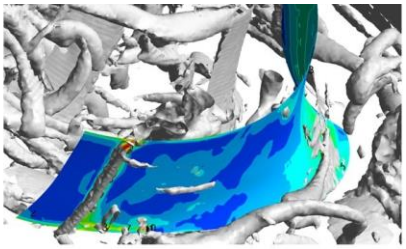

Fig. 13 vortex core near surface S4 at 50%Pn of turbine operation fig. 14 vortex core near surface S5 at 50%Pn of turbine operation

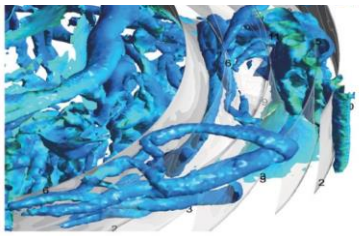

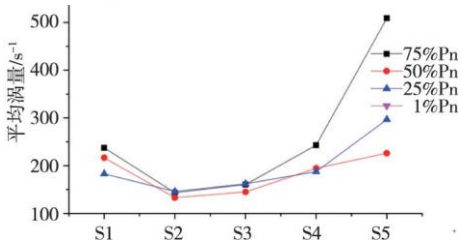

Figure 15 Turbine Working Condition, 50%Pn and Vortex Core Region Map of Vortex in Lower One Blade Path 16 Virtual Surface Average Vorticity of Turbine Off-design Working Condition

Limited by measurement and analysis methods, the research on vortex system is still limited. The shape and function of various vortex structures are not identical.

Similarly, for example, the claw vortex is also called vertical vortex, spiral vortex, tornado vortex, etc., which is the result of three-dimensional separation in flow. The shape of the claw vortex surface is a separation spiral point and a tornado shape. The cornucopia vortex has higher frequency, smaller structural scale and weaker vortex strength, but it shows its hydrodynamic effect and influence on the development of the main vortex system through the main vortex.

When studying turbulence, people often pay attention to the development of the main vortex system and seldom observe or notice the existence and characteristics of the claw vortex. Tubular vortex is the result of the development of flow structure in the blade passage space. As the tubular vortex is a twisted vortex structure with a circumferential component, and its shape is like a water tube through the stretching of adjacent blade walls, which is difficult to capture

in general numerical calculation, it is rarely mentioned in the literature. The tubular vortex captured in this paper is located in the middle of the blade passage and disappears at the exit of the blade passage. The horseshoe vortex is relatively strong, and its formation mechanism is relatively single compared with that of tubular vortex. It is easy to capture in numerical calculation. Some scholars have done a lot of research on horseshoe vortex in planar two-dimensional flow field, such as Chen Qigang.

Horseshoe vortices generated by equicylindrical flows have been studied, but horseshoe vortices in three-dimensional twisted space are still rarely reported. Adilozturk etc

For "spiral streamline is the main basis for judging the existence of horseshoe vortex and determining the position and shape of horseshoe vortex. vortex structure has spiral rotation

Features ". According to the streamline distribution characteristics, the location of horseshoe vortex in this calculation is determined as shown in figure 17 and figure 18 , which is similar to the figure

The positions of horseshoe vortex captured in 5 and 7 are consistent. But Jeong and so on. It is believed that the shape of streamline changes with the observation coordinate system, namely

Streamlines do not satisfy Galileo invariance, so vortex structures identified by streamline method are not of universal significance ". Referring to the results of two-dimensional space research,

In order to ensure that the identified vortex structure not only has spiral streamline characteristics, but also satisfies Galileo invariance in geometry, rotation intensity λ and c_I are defined as horseshoe vortex identification variables.

Let the velocity gradient matrix of any point in the three-dimensional flow field be:

It is the rotational strength, and its size reflects the strength of the vortex structure. However, it is necessary to prove

When the velocity gradient matrix has complex characteristic roots, the flow field around it is spiral ".

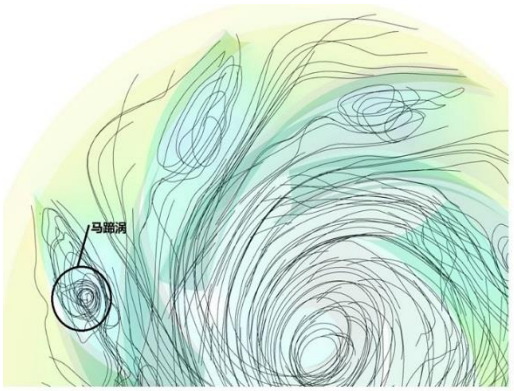

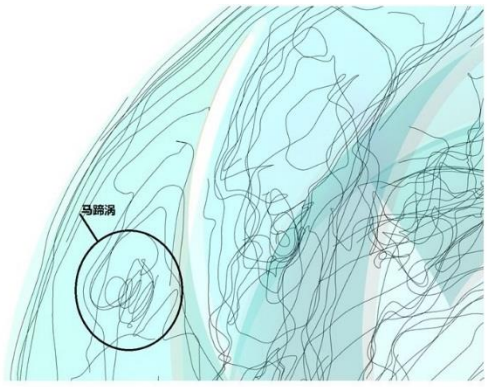

Fig. 17 internal flow line of 50%Pn runner for hydraulic turbine operation fig. 18 internal flow line of 1%Pn runner for hydraulic turbine operation

The strong unsteady multi-vortex system produces great shear stress and scouring collision in the blade passage, which increases the energy dissipation and increase

Resistance of fluid machinery, causing greater flow energy loss, reducing fluid machinery efficiency, enhancing flow noise and mechanical vibration. When the vortex system is asymmetric, a large lateral force and eccentric moment will be induced on the runner. This is also an unstable and complicated flow structure change that often leads to the instability of the unit. In light of this, the noise of the factory building increases, the vibration swing of the unit increases, the active power mutation, frequent micromotion of the governor relay, unsuccessful grid connection, etc., while in heavy cases, it is one of the important hydraulic factors that cause the unit accident. For example, the injected stator one-point grounding protection power supply contact of 4 generator (600 MW) of a cascade power station in Yunnan province looses due to long-term no-load vibration, resulting in tripping of the protection unit. Therefore, precautions should be taken in engineering practice. 3.2 Transition Process of Increasing Flow Rate in Pump Operation Flow Line in 1 %Pn Flow Channel of Pump Operation is shown in Figure 19, and Vortex Core in Flow

Channel of Each Pump Operation is shown in Figure 20- and Figure 24. When the pump turbine is operating in the small flow area under the pump condition, the water flow in the draft tube is stable, and after entering the runner, it collides with the inlet edge of the blade to generate a vortex structure, and generates a vortex belt near the outlet edge of the blade (see fig. 19—-fig. 20). As the streamline in the congested blade passage rises spirally, the water flows out of the rotating wheel and enters the water guiding mechanism; Due to the narrow flow passage between the movable guide vanes, the water flow cannot pass quickly, resulting in backflow phenomenon, and a series of vortex structures are generated due to the shedding of flow at the tail end of the movable guide vanes. The vortex structure collapses in large quantities between the fixed guide vanes as the water flows to the volute. Compared with other flow area conditions under the pump condition, the inlet water flow of the runner and the inlet edge of the blade have a larger attack angle when the pump operates in the small flow area, resulting in impact and serious flow shedding.

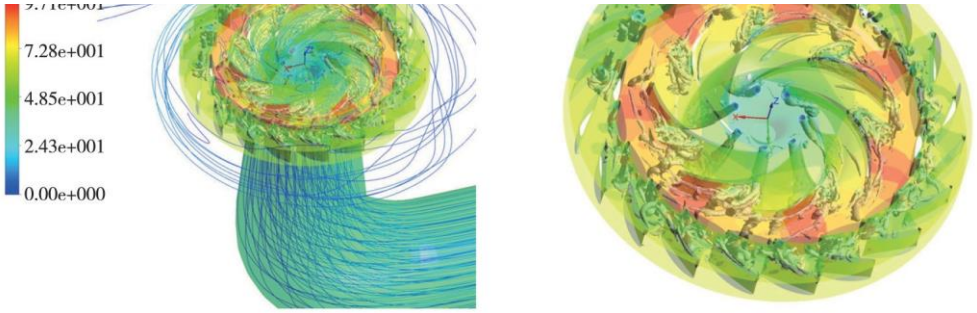

Fig. 19 flow line in 1%Pn flow channel under water pump condition fig. 20 vortex core in 1%Pn flow channel under water pump condition

As the opening of the movable guide vane increases, the water flow increases, the flow pattern tends to be more stable, the streamline is smooth and uniform, and the streamline does not

Again in a spiral shape, but still a small amount of moving vane wake can be observed. With the further increase of the flow, due to the congestion of the flow, the flow lines are becoming more uneven and irregular. Streamlines in the draft tube are intertwined with each other, and there is a rotating component in the water flow. The flow line in the rotating channel is similar to that in the case of small flow rate and rises spirally. And there is a small amount of vortex structure in elbow section of draft tube. In addition, a large number of vortex structures are generated due to impact near the inlet side of the runner blade pressure surface near the lower ring side, and part of the fluid reversely flows

into tail water along the side wall of the draft tube under the action of the vortex structures

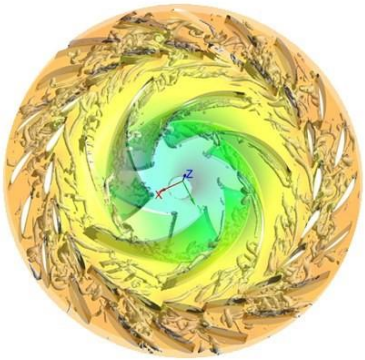

Figure 21

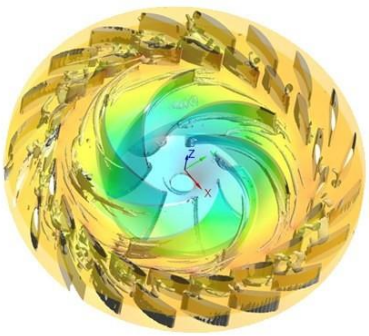

Figure 22

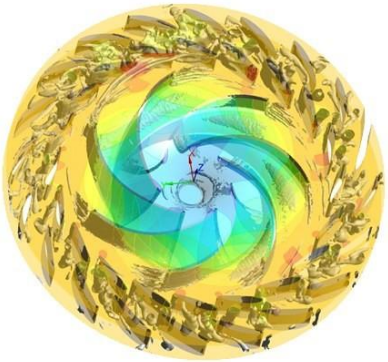

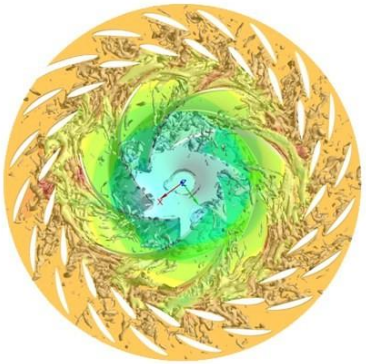

Fig. 23 vortex core in 75%Pn flow channel under water pump condition fig. 24 vortex core in 100%Pn flow channel under water pump condition

The reverse flow of the tube and the circumferential outer flow passage on the side of the lower ring forms a separation vortex.

There are relatively few vortex structures in the runner under pump operation, and the vortex structures in the water guide mechanism area vary greatly. As shown in Figure 25—-Figure 29 , it is the vorticity (absolute value) of the central section of the water guide mechanism under each water pump condition, and as shown in Figure 30 , it is the average vorticity of the central section of the water guide mechanism. This shows that water

The absolute value of vorticity of the water guide mechanism is the largest under the pump working condition of 100 %Pn, the smallest under the pump working condition of 1 %Pn, and the other working conditions are in the middle. The absolute value of vorticity of water guide mechanism is greatly affected by flow congestion when the pump is operating at 100% Pn, while the most important influencing factor comes from wall viscosity when the pump is operating at 1 %Pn.

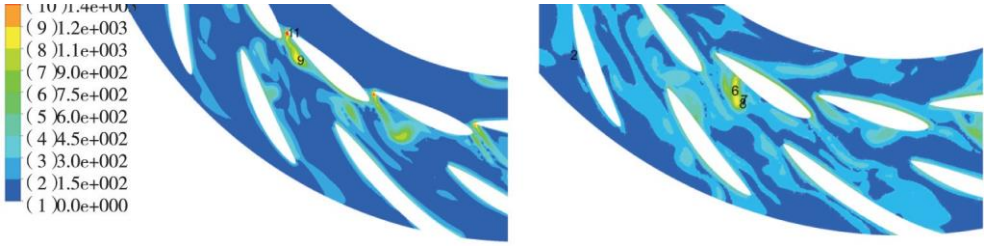

Figure 25 Pump Working Condition, 1%Pn and Water Conductor Vorticity of central section

Figure 26 Pump Working Condition, 25%Pn and Water Conductor

Vorticity of central section

Compared with the pump condition, the turbine condition has the highest amount of vortex in the runner, with more obvious vortex system development, more vortex structures and most distribution.

In the front half of the blade path, it changes obviously with the opening of the guide vane. As shown in fig. 30 , the average vorticity of the water guide mechanism under the pump condition is higher than that under the corresponding hydraulic turbine condition. In addition, the average vorticity of the pump is the largest under rated working conditions and the smallest under no-load conditions. On the other hand, the average vorticity is the largest when the turbine is operating at no load. In the water guide mechanism area, the turbine operating vortex structure changes little, and it is not easy to observe the vortex structure, while the pump operating vortex structure is more and changes obviously with the guide vane opening.

The above analysis shows that the characteristics of vortex structures in the runner region and the water guide mechanism region are basically opposite for the pump and turbine operating conditions, but there are commonness, i.e. water flows from large space to small space, flow passages are blocked, vortex structures increase and change significantly; On the contrary, the flow passage is smoother and the vortex structure changes are not obvious and relatively less.

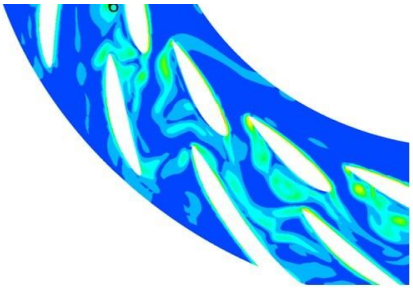

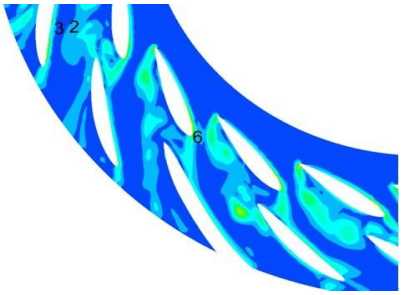

Figure 27 Pump Working Condition, 50%Pn and Water Conductor Vorticity of central section

Figure 28 Pump Working Condition, 75%Pn and Water Conductor Vorticity of central section

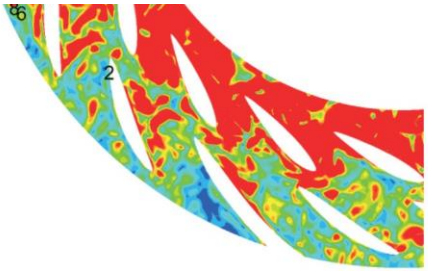

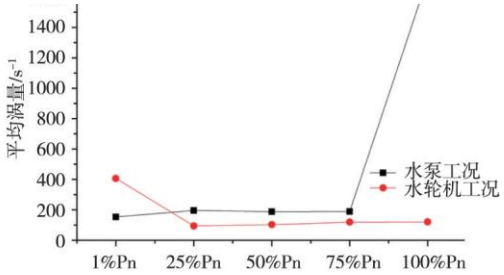

Figure 29 Pump Working Condition, 100%Pn, Vorticity Diagram of Central Section of Water Conductor 30 Average Vorticity of Central Section of Water Conductor

Conclusion

In this paper, the large eddy simulation method based on Smagorinsky-Lilly sub-grid stress model is adopted to carry out three-dimensional unsteady turbulent numerical calculation on the transition process of load increase and decrease from rated turbine condition to rated pump condition. The unsteady flow structure in the small flow area of turbine condition and water pump condition is analyzed emphatically, and the main factors of great changes in flow pattern are explored. According to the analysis and research, the following conclusions are drawn:

(1) Because the inlet flow velocity of the runner is not consistent with the tangential direction of the inlet blade's bone line, there is an angle of attack. The water flows into the blade passage along the inner arc and back arc of the blade after passing through the obstruction of the blade leading edge. Under the joint influence of the viscous effect of the three-dimensional twisted blade curved surface and the reverse pressure gradient caused by the protrusions, the boundary layer flow develops on the curved surface to generate three-dimensional flow separation, forming shedding. The shedding vortex forms a complex vortex system in the blade passage, namely the blade passage vortex. The calculation captured the tubular vortex developed in the blade path.

(2) The vortex system structure induced by different attack angles of water flow inlet is also different. When the angle of attack is small, the rupture of the tubular vortex will cause the spiral vortex to develop into a claw vortex in the blade passage. When the angle of attack is large, it develops into horseshoe vortex. When the angle of attack is medium, both claw vortex and horseshoe vortex are formed in the blade passage. The higher the angle of attack, the more complex the vortex system is.

(3) When the turbine works, the average vorticity near the blade wall is large and the suction surface is higher than the pressure surface. The flow separation is relatively significant, followed by the middle of the flow passage. The smaller the opening of the guide vane, the greater the energy loss of the vortex structure.

(4) Vortex structure in the water guide mechanism region changes significantly with the opening degree under the pump condition, and its average vorticity is higher than that under the corresponding turbine condition. In addition, the average vorticity of the water pump is the largest under rated conditions and the smallest under no-load conditions. On the other hand, the average vorticity is the largest when the turbine is operating at no load. Water flows from large space to small space, the flow passage is blocked, vortex structure increases and changes significantly; On the contrary, the flow passage is smoother and the vortex structure changes are not obvious and relatively less.

References

1. Li Jun, Chloe Wang, Liao Weili. Analysis of internal flow field characteristics in "S" shaped region of reversible pump turbine [J]. Journal of Agricultural Engineering, 2014,30 (15):106-113 .
2. You Guanghua, Kong Linghua, Liu Deyou. The "S" shape characteristics and countermeasures of pump turbine in Tianhuangping Pumped Storage Power Station [J]. Journal of Hydroelectric Power Generation, 2006.25（6）：136-139 .
3. LIU J T，LIU S H，SUN Y K，et al . Numerical simulation of pressure fluctuation of a pump-turbine with MGV at no-l oad condition［C］//IOP Conference Series：Earth and Environmental Science.［S.L.］：IOP Publishing，2012 .
4. XIAO Y X，XIAO R F . Transient simulation of a pump - turbine with misaligned guide vanes during turbine mod‐el start-upXZ80 05J］. Acta Mechanica Sinica，2014，30（5）：646-655 .
5. Tao Ran, Xiao Ruofu, Yang Wei, et al. . Hump Characteristics of Reversible Pump Turbine Pump Working Conditions [J ］. Journal of Irrigation and Drainage Mechanical Engineering, 2014，32（11）：927-930 .
6. Wang Huanmao, Wu Gang, Wu Weizhang, et al. . Numerical Simulation and Analysis of Hump Region of Francis Pump Turbine [J ］. Journal of Hydroelectric Power Generation, 2012，31（6）：253-258 .
7. HASMATUCHI V，FARHAT M，ROTH S，et al . Experimental evidence of rotating stall in a pump-turbine at off-design co nditions in generating mode［J］. Journal of Fluids Engineering，2011，133（5）：051104 .
8. Xia Linsheng, Cheng Yongguang, Cai Fang, et al. . Numerical Analysis of Flow Characteristics in Four Quadrant Working Area of Pump Turbine [J ］. Journal of Water Conservancy, 2015，46（7）：859-868 .
9. Zhang Yaoliang, Zhu Weibing . Tensor Analysis and Its Application in Continuum Mechanics [m ］. Harbin: Harbin Engineering University Press ".2004：198-219 .
10. Wu Yulin, Liu Shuhong, Qian Zhongdong . Hydromechanical Computational Fluid Dynamics [M ］. Beijing: China Water Resources and Hydropower Publishing House, 2007.
11. Wang Fujun. Computational Fluid Dynamics Analysis-Principles and Applications of -CFD Software [M]. Beijing: Tsinghua University Publishing House, 2004.
12. MENEVEAU C，KATZ J . Scale-invariance and turbulence models for large-eddy simulation［J］. Annual Review of Fluid Mechanics，2000，32：1-32 .

13. REBOLLO T C，LEWANDOWSK R . A variational finite element model for large-eddy simulations of turbulent flows［J］. Chinese Annals of Mathematics，（Series B），2013，34（5）：667-682 .
14. Guo Tao, Zhang Lixiang . Study on Turbulent Characteristics and Blade Vortex Structure in Guide Mechanism of Francis Turbine with Small Opening [J ］. Engineering Mechanics, 2015，32（6）：222-230 .
15. Chen Qigang, Qi Meilan, Li Jinzhao . Study on Kinematic Characteristics of Horseshoe Vortex Upstream of Open Channel Column [J ］. Journal of Water Conservancy, 2016，47（2）： 158-164.
16. ADILOZTURK N，AKKOCA A，SAHIN B . Flow details of a circular cylinder mounted on a flat plate［J］. Jour‐ na l of Hydraulic Research，2008，46（3）：344-355 .
17. JEONG J，HUSSAIN F . On the identification of a vortex［J］. Journal of Fluid Mechanics，1995，285：69-94 .